
μ Mist[®]

- ▶ [Spray Technologies Inspired by Bombardier Beetle](#)

μ VED (Micro Vacuum Electronic Devices)

- ▶ [MEMS Vacuum Electronics](#)

193-nm Lithography

- ▶ [DUV Photolithography and Materials](#)

248-nm Lithography

- ▶ [DUV Photolithography and Materials](#)

3D Micro/Nanomanipulation with Force Spectroscopy

H. Xie¹ and Stéphane Régnier²

¹The State Key Laboratory of Robotics and Systems, Harbin Institute of Technology, Harbin, China

²Institut des Systèmes Intelligents et de Robotique, Université Pierre et Marie Curie, CNRS UMR7222, Paris, France

Synonyms

[Force spectroscopy](#); [Nano manipulation](#); [Nanorobotics](#)

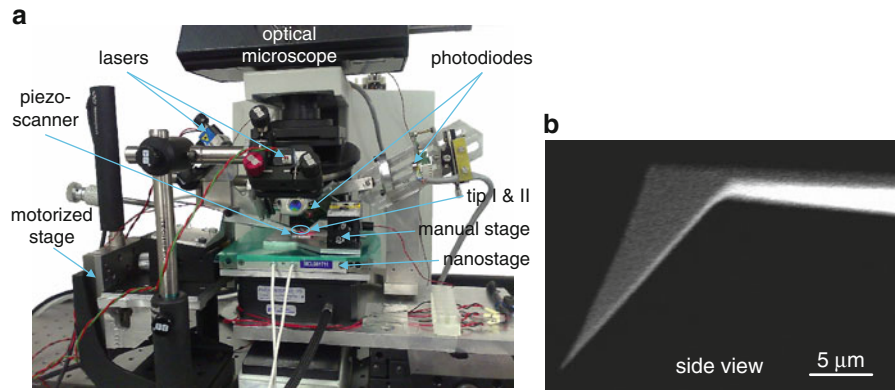
Definition

A micromanipulation system is a robotic device which is used to physically interact with a sample under a microscope, where a level of precision of movement is necessary that cannot be achieved by the unaided human hand

It is well known that pick-and-place is very important for 3-D microstructure fabrication since it is an indispensable step in the bottom-up building process. The main difficulty in sufficiently completing such pick-and-place manipulation at this scale lies in fabricating a very sharp end-effector that is capable of smoothly releasing microobjects deposited on the substrate. Moreover, this end-effector has to provide enough grasping force to overcome strong adhesion forces [1–3] from the substrate as well as being capable of sensing and controlling interactions with the microobjects. Furthermore, compared with the manipulation of larger microobjects under an optical microscope, visual feedback at several microns more suffers from the shorter depth of focus and the narrower field of view of lenses with high magnifications, although different schemes or algorithms have been introduced on techniques of autofocusing [4, 5] and extending focus depth [7]. Compared with vision-based automated 2-D micromanipulation, automated 3-D micromanipulation at the scale of several microns to submicron scale is more challenging because of optical microscope's resolution limit (typically 200 nm). Moreover, additional manipulation feedback is needed that is beyond the capability of optical vision, such as in the cases of vertical contact detection along the optical axis or manipulation obstructed by opaque components. Therefore, multi-feedback is of vital

3D Micro/ Nanomanipulation with Force Spectroscopy,

Fig. 1 (a) A photo of the AFM-FRS on the configuration for nanoscale pick-and-place manipulation. (b) A SEM image of the cantilever fabricated with a protruding tip



importance to achieve such accurate and stable 3-D micromanipulation at the scale of several microns to submicron scale.

Pick-and-place nanomanipulation is also a promising technique in 3D nanostructure fabrication since it is an indispensable step in the bottom-up building process. It can overcome limitations of bottom-up and top-down methods of nanomanufacturing and further combine advantages of these two methods to build complex 3D nanostructures. In literature, nanostructures have been manipulated, assembled, and characterized by integrating nanomanipulators or nanogrippers into scanning electron microscopes (SEM) and transmission electron microscopes (TEM) [12–16]. Both the SEM and the TEM provide a vacuum environment where the van der Waals force is the main force to be overcome during the manipulation. 3D nanomanipulation could be also achieved with optical tweezers in liquid, where the adhesion forces are greatly reduced [17–19]. However, the pick-and-place nanomanipulation in air is still a great challenge due to the presence of strong adhesion forces, including van der Waals, electrostatic and capillary forces [20]. In this case, the main difficulties in achieving the 3D nanomanipulation are fabricating sharp end-effectors with enough grasping force, as well as capabilities of force sensing while controlling interactions between the nanoobject and the tool or the substrate.

In this entry, a concept is presented to make a prototype of an AFM-based flexible robotic system (FRS) which is equipped with two collaborative cantilevers. By reconfiguring the modular hardware and software of the AFM-FRS, different configurations can be obtained. With different manipulation strategies

and protocols, two of the configurations can be respectively used to complete pick-and-place manipulations from the microscale of several microns to the nanoscale that are still challenges.

This entry is organized as follows. Section I introduces the prototype and experimental setup of the AFM-FRS. In subsection II and III, pick-and-place manipulation of microspheres and nanowires for building 3-D micro/nano structures are performed using the AFM-FRS.

AFM-Based Flexible Robotic System

AFM-FRS Setup

Figure 1a shows the AFM-FRS system setup, which is in the configuration for nanoscale pick-and-place. The system is equipped with an optical microscope and two sets of modules commonly used in a conventional AFM, mainly including two AFM cantilevers (namely, tip I and tip II, ATEC-FM Nanosensors, see Fig. 1b), two sets of nanopositioning devices and optical levers. The motion modules include an open-loop X - Y - Z piezoscanner (PI P-153.10H), an X - Y - Z closed-loop nanostage (MCL Nano-Bio2M on the X - and Y -axis, PI P-732. ZC on the Z -axis), an X - Y - Z motorized stage, and an X - Y - Z manual stage. Detailed specifications of the motion modules are summarized in Table 1. Figure 1c shows an optical microscope image of the collaborating tips in microsphere grasping mode.

A data acquisition (NI 6289) card is used for high-speed (500~800 Hz of sampling frequency for force and 600 kHz for amplitude) capture of the photodiode voltage output to estimate deflections on both tips induced by force loading or resonant oscillation.

3D Micro/Nanomanipulation with Force Spectroscopy,**Table 1** Specifications of each motion module

Actuator	Travel range	Resolution
X-Y-Z piezoscanner	10 × 10 × 10(μm)	Sub-nm
X-Y-Z nanostage	50 × 50 × 10(μm)	0.1 nm
X-Y-Z motorized stage	25 × 25 × 25(mm)	50 nm
X-Y-Z manual stage	5 × 5 × 5(mm)	0.5 μm

A multi-thread planning and control system based on the C⁺⁺ is developed for AFM image scan and two-tip coordination control during manipulation. This control system enables programming of complex tasks on the highly distributed reconfigurable system.

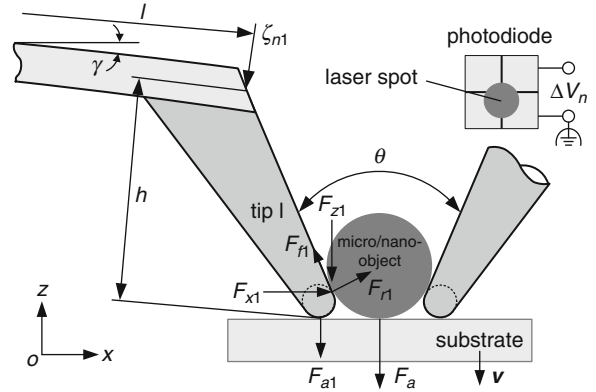
Force Sensing During Pick-and-Place

Figure 2 shows a schematic diagram of the nanotip gripper for the micro/nanoscale pick-and-place operation that has a clamping angle $\theta \approx 44^\circ$ micro/nanoscale pickup manipulation, for instance, interactive forces applied on tip I include repulsive forces F_{r1} , friction forces F_{f1} , and adhesive forces F_{a1} .

The forces applied on tip I can be resolved into two components on the X-axis and the Z-axis in the defined frame, namely, F_{x1} and F_{z1} , respectively. F_{x1} is the clamping force that holds the micro/nanoobject. F_{z1} is the pickup force that balances adhesion forces from the substrate. To sense the pickup force, it is necessary to know the normal deflection on both cantilevers. The normal deflection ζ_{n1} associated with the normal voltage output of the optical lever on tip I is given by:

$$\zeta_{n1} = \frac{F_{z1} \cos \gamma + F_{x1} \sin \gamma}{k_n} + \frac{F_{z1} \sin \gamma + F_{x1} \cos \gamma}{k_{xz}} \quad (1)$$

where γ is the mounting angle of the cantilever, $k_{xz} = 2lk_n/3h$ is the bending stiffness due to the moment applied on the tip end, where h is the tip height. Assuming the magnitude of F_{z1} and F_{x1} are of the same order, contributions from the F_{x1} to the normal deflection of tip I are relatively very small since $k_{xz} \gg k_n$ and $\gamma = 5^\circ$. Therefore, the normal deflection induced from F_{z1} is only considered in the following calculations of the adhesion force F_a applied on the micro/nanoobject. Thus, F_{z1} can be simplified by estimating the normal voltage output ΔV_{n1} from the tip I:



3D Micro/Nanomanipulation with Force Spectroscopy, Fig. 2 Schematic diagram of the nanotip gripper and force simulation during the pickup manipulation

$$F_{z1} = \beta_1 \times \Delta V_{n1} \quad (2)$$

where β_1 is the normal force sensitivity of the optical lever. A similar pickup force F_{z2} can be also obtained on Tip II. Before the gripper pulls off the substrate, the adhesion force F_a can be estimated as:

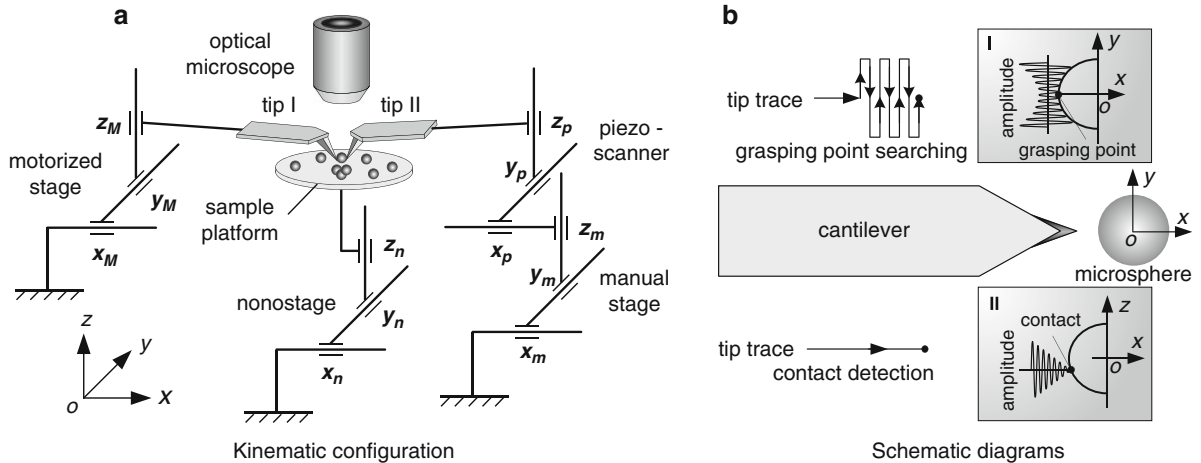
$$F_a = F_{z1} + F_{z2} = \beta_1 \Delta V_{n1} + \beta_2 \Delta V_{n2} - (F_{a1} + F_{a2}) \quad (3)$$

where β_2 , ΔV_{n2} , and F_{a2} are respectively the normal force sensitivity, normal voltage output, and adhesive force on tip II. Once the gripper pulls off the substrate, e.g., in the case of nanowire/tube pick-and-place, the adhesion force F_a is estimated as:

$$F_a = F_{z1} + F_{z2} = \beta_1 \Delta V_{n1} + \beta_2 \Delta V_{n2}. \quad (4)$$

Experimental Results**3-D Micromanipulation Robotic System****System Configuration for 3-D Micromanipulation**

As the size of microobjects is reduced to several microns or submicrons, problems will arise with these conventional grippers: (1) Sticking phenomena becomes more severe due to the relatively larger contact area between the gripper and the microobject. (2) The tip diameters of the micro-fabricated clamping jaws are comparable in size to the microobjects to be grasped. Conventional grippers are not geometrically



3D Micro/Nanomanipulation with Force Spectroscopy, Fig. 3 A kinematic configuration and schematic diagrams for 3-D micromanipulation at a scale of several micrometers or

sharp enough to pick up microobjects of several micrometers deposited on the substrate. Fortunately, the AFM tip has a very tiny apex (typically ~ 10 nm in radius) with respect to the size of the microobject to be manipulated. Thus, the nanotip gripper can be used to achieve pick-and-place at the scale of several microns since the contact area of the gripper-microobject is much smaller than the microobject-substrate contact. Moreover, real-time force sensing makes the manipulation more controllable.

As shown in Fig. 3, the system configuration for 3-D micromanipulation is reconfigured as follows:

1. For a large manipulation travel range, the nanostage here is used to support the sample platform and transport the microobject during the manipulation.
2. Tip I, immovable during the pick-and-place micromanipulation, is fixed on the motorized stage for coarse positioning.
3. Tip II is actuated by the piezoscanner for gripper opening and closing operations. The piezoscanner is supported by the manual stage for coarse positioning.

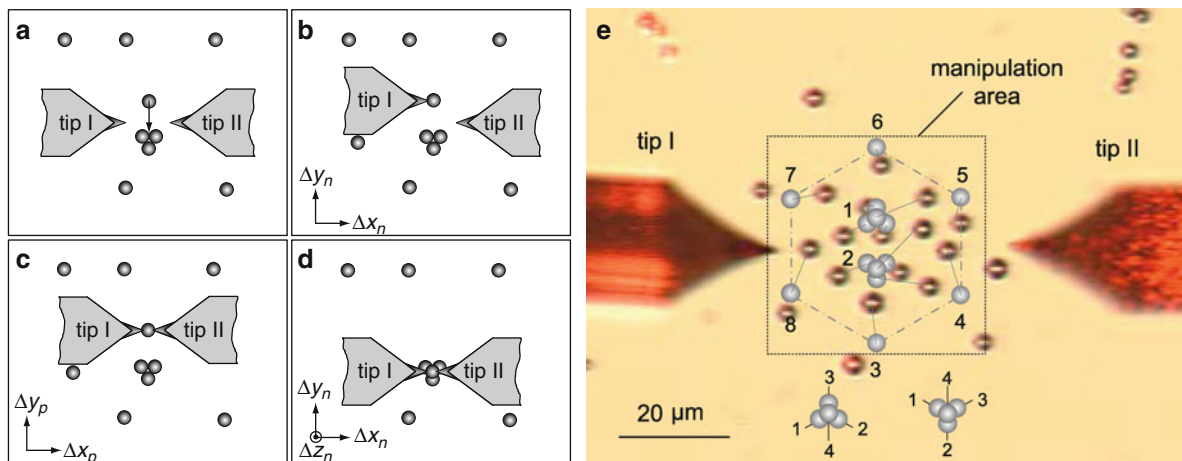
Benefiting from AFM-based accurate and stable amplitude feedback of a dithering cantilever, the grasping state can be successfully achieved by the amplitude feedback, with very weak interaction at the nano-Newton scale, protecting the fragile tips and the microobjects from damage during manipulation. As shown in inset I of Fig. 3, the dithering cantilever with its first resonant mode is used to locate

grasping point searching (inset I) and contact detection (inset II) with amplitude feedback of the dithering cantilever

grasping points and detect contact. When approaching the microsphere with a separation between the tip and the substrate (typically 500 nm), the tip laterally sweeps the microsphere over the lower part of the microsphere. By this means, the grasping point can be accurately found by locating the minimum amplitude response of each single scan.

From the scheme depicted in inset II of Fig. 3, the amplitude feedback is also used for contact detection. Tip-microsphere contact is detected as the amplitude reduces to a steady value close to zero. As shown in Fig. 4, a protocol for pick-and-place microspheres mainly consists of four steps:

- System initialization and task planning: Each axis of the nanostage and the piezoscanner are set in a proper position, supplying the manipulation with enough travel range on each axis. Then the task is planned in Fig. 4a with a global view of the manipulation area that provides coarse positions of the microspheres and tips.
- Making tip I-microsphere in contact: In Fig. 4b, tip I has started to approach the microsphere by moving the nanostage with amplitude feedback to search for the grasping point and detect contact.
- Forming the gripper: Similarly, tip II approaches the microsphere by moving the piezoscanner. Once tip II and the microsphere are in contact, a nanotip gripper is configured in Fig. 4c for a manipulation.
- Pick-and-place micromanipulation: In Fig. 4d, the microsphere is picked up, transported, and released



3D Micro/Nanomanipulation with Force Spectroscopy, Fig. 4 Microsphere manipulation protocol. (a) Task planning. (b) Tip I and the microsphere are in contact. (c) The nanotip

by moving the nanostage with a proper displacement on each axis that depends on the diameter of the microsphere and its destination. The whole process of 3-D micromanipulation is monitored by real-time force sensing.

3-D Microsphere Assembly

Nylon microspheres with diameter of about $3 \sim 4 \mu\text{m}$ were manipulated to build 3-D microstructures in experiments. The microspheres were deposited on a freshly cleaned glass slide and then an area of interest was selected under the optical microscope. Figure 4 shows a plan view of the selected area, in which 14 microspheres separated in a $50 \mu\text{m}$ square frame are going to be manipulated to build two 3-D micropylramids and a regular 2-D hexagon labeled by assembly sequences from 1 to 8. Each pyramid is constructed from four microspheres with two layers and the assembly sequences are shown in the bottom insets for two different arrangements of the pyramids.

Figure 5 shows a result of grasping point searching, in which the dithering tip II laterally sweeps the microsphere within a range of $1.75 \mu\text{m}$ on the y -axis and with a free oscillating amplitude of about 285 nm . Ten different distances to the microsphere were tested from 100 to 10 nm with an interval of 10 nm and, consequently, the grasping point is well located with an accuracy of $\pm 10 \text{ nm}$. Figure 5 shows a full force spectroscopy curve during the pick-and-place of a microsphere deposited on a glass slide with an ambient temperature of 20°C and relative humidity of 40%.

gripper is formed. (d) Pick up and release the microsphere to its target position. (e) Task descriptions of the microsphere assembly

In this curve, point A represents the start of the pick-and-place, point B the pull-off location of the microsphere-substrate contact, point C nonlinear force restitution due to the tip-microsphere frictions, and point D the snap-in point between the microsphere and the substrate. The force spectroscopy curve is synthesized from force responses on tip I and tip II.

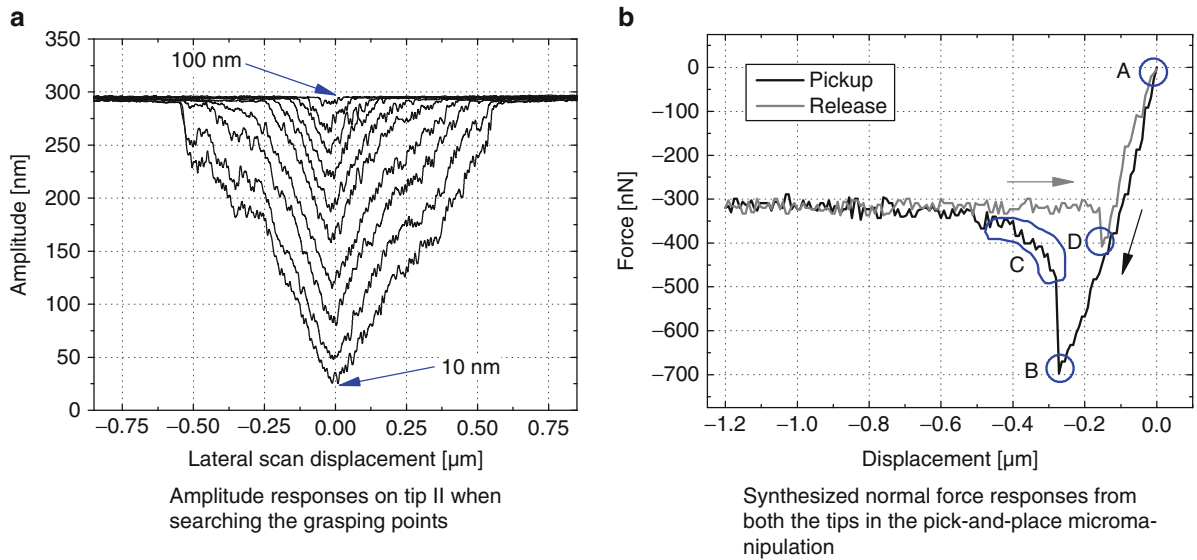
Figure 6 shows an automated microassembly result consisting of two 3-D micropylramids and a 2-D pattern of a regular hexagon. The whole manipulation process was completed in 11 min, so the average manipulation time for each microsphere is about 47 s, which mainly breaks down into about 20 s for microsphere grasping including the grasping point search and contact detection processes using amplitude feedback, $10 \sim 35 \text{ s}$ for microsphere release and, the remaining time for transport.

Assembly of the fourth is the key to success in building a micropylramid. During pick-and-place of the fourth microsphere, microscopic vision was firstly used for coarse positioning it target, then the normal force feedback of the gripper was used to detect the vertical contact between the fourth microsphere and other three microspheres on the base. When the contact is established, a small vertical force was applied on the fourth microsphere by moving the nanostage upward and it will adjust to contact with all the base microspheres.

3-D Nanomanipulation Robotic System

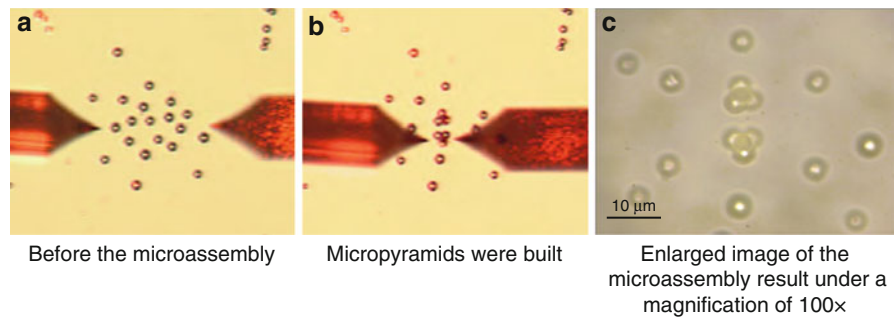
System Configuration for 3-D Nanomanipulation

Compared with the 3-D micromanipulation, tip alignment precision is the key factor in succeeding the



3D Micro/Nanomanipulation with Force Spectroscopy, Fig. 5 Experimental results

3D Micro/Nanomanipulation with Force Spectroscopy, Fig. 6 A microassembly result



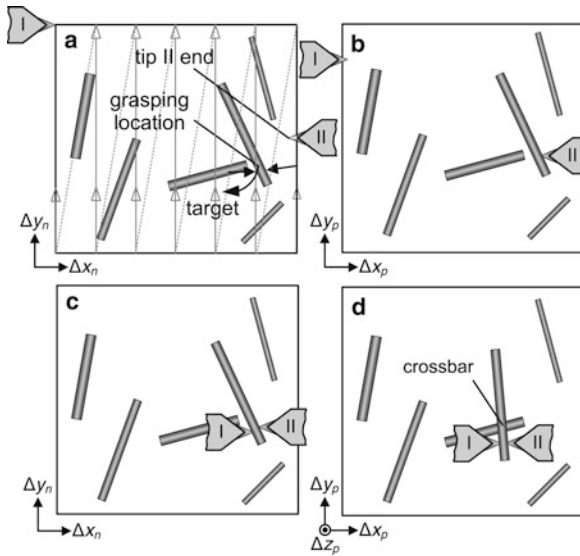
nanoscale pick-and-place. Therefore, the closed-loop nanostage is considered in this configuration for accurate tip alignment. As shown in Fig. 7, the system configuration for 3-D nanomanipulation is reconfigured as follows:

1. The nanostage is used for image scan with tip I.
2. Nanoobjects are supported and transported by the piezoscanner.
3. Tip I, fixed on the motorized stage for coarse positioning, is immovable during the pick-and-place micromanipulation. Before manipulation, cantilever I acts as an image sensor for nanoobject positioning.
4. For accurate gripper alignment between Tip I and Tip II, Tip II is fixed on the nanostage rather than the piezoscanner. Tip II is supported by the manual stage for coarse positioning.

Nanowires and nanotubes are being intensively investigated. Thus, a protocol is developed here for nanowire or nanotube pick-and-place. However, applications can easily be extended to, for example, pick-and-place of nano-rods or nanoparticles dispersed on a substrate.

Once the manipulation area is selected under the optical microscope, both the tips are aligned as a quasi-gripper above the center of the manipulation area. Each axis of the nanostage and the piezoscanner is initialized at an appropriate position to allow for enough manipulation motion travel.

In this step, tip I is used to fully scan the relevant area obtaining a topographic image that contains nanoobjects to be manipulated and the end of tip II. Figure 7a shows a simulated image that contains the topography of two nanowires and the end of tip II. The image provides the following pick-and-place with



3D Micro/Nanomanipulation with Force Spectroscopy, Fig. 7 A protocol for nanowire pick-and-place (a) Image scan for task planning. (b) Tip II is in contact with the nanowire. (c) Tip I is in contact with the nanowire, forming a nanotip gripper. (d) Pick up and release a nanowire to its target position (e) A kinematic configuration of the AFM-RFS for nanoscale pick-and-place

relative positions between tip I, tip II and the nanoobjects to be manipulated. However, after a long period image scan, relocating tip II is recommended to eliminate system's thermal drift.

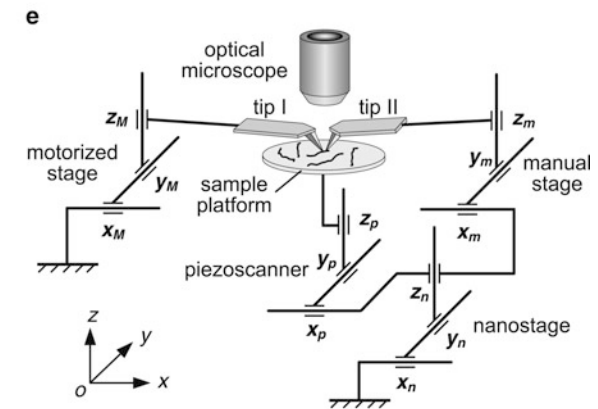
As shown in Fig. 7b, tip II approaches the nanowire to make contact by moving the X-axis of the piezoscanner. A gap (typically ~ 20 nm above the snap-in boundary) between Tip II and the substrate should be maintained during the approach to enable a negative deflection response in the form of a tiny force applied on tip II, and hence, sensitive detection of the tip-nanowire contact.

Similarly, in Fig. 7c, once tip I is in contact with the nanowire, a nanotip gripper is configured for pick-and-place manipulation of the nanowire.

The nanotip gripper in this step is used to pick up, transport, and release the nanowire to its target position by moving the piezoscanner on the X, Y, or Z-axis. The displacement on each axis depends on the dimensions of the nanowire and the location of the destination. Figure 7d shows a simulated post-manipulation image, in which a nanowire crossbar is built. The complete pick-and-place procedure is monitored by force sensing.

Pick-and-Place Nanomanipulation

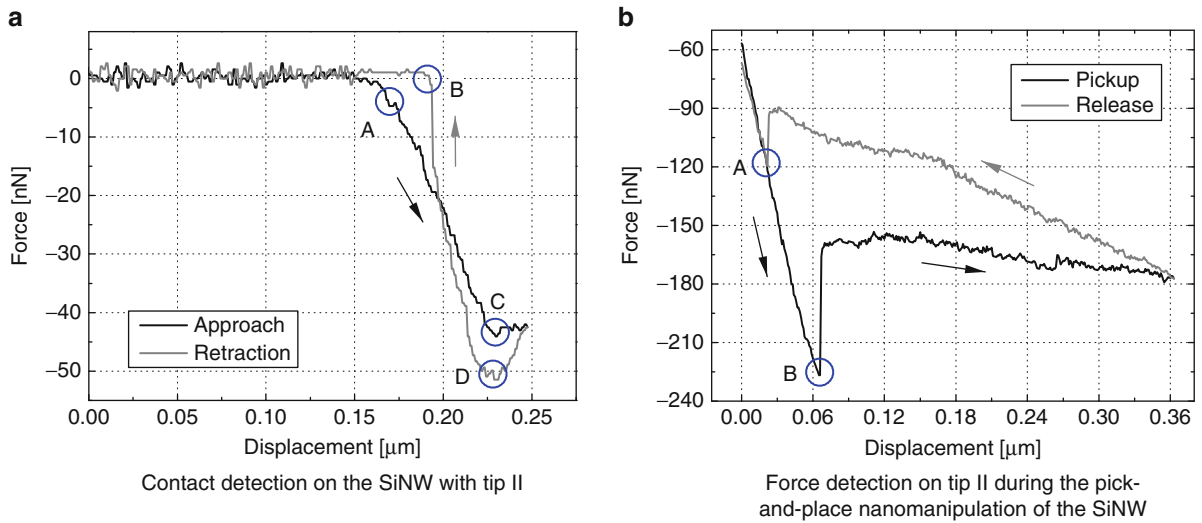
In experiments, silicon nanowires (SiNWs) were deposited on a freshly cleaned silicon wafer coated



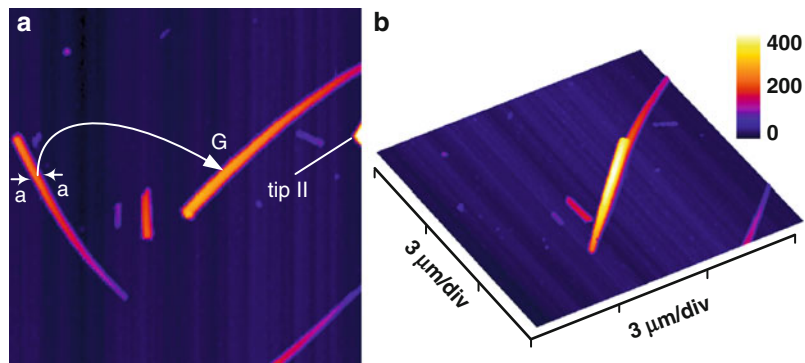
with 300 nm silicon dioxide. AFM images show that the SiNWs have a taper shape and have diameters of 25 nm (top), ~ 200 nm (root), and lengths of about $4 \sim 7$ μm .

Figure 8 shows an example of the contact detection with tip II: Point A and point C are where the tip contacts with the SiNW and the Si substrate, respectively; Point B and point D are where the tip breaks the contact with the Si substrate and the SiNW, respectively. Figure 8 shows a curve of the peeling force spectroscopy on tip II for the pick-and-place manipulation of the SiNW: point A and point B are where the tip snaps in and pulls off the Si substrate, respectively. The shape of curve of the force responses on tip I are similar except for the force magnitude due to different force sensitivities on each tip and uneven grasping due to asymmetric alignment of the SiNW relative to the grasping direction. This force spectroscopy during the pickup operation shows stable grasping for further SiNW transport.

Figure 9 shows an experimental result of 3-D SiNW manipulation. A prescanned image (9×9 μm) is shown in Fig. 9a, which includes the topographic image of SiNWs and the local image of tip II. A grasping location of the nanowire to be manipulated is marked with a-a, where the SiNW has a height of 160 nm. Figure 9b is a post-manipulation image. It can



3D Micro/Nanomanipulation with Force Spectroscopy, Fig. 8 Contact and force detection



3D Micro/Nanomanipulation with Force Spectroscopy, Fig. 9 Pick-and-place results of the SiNWs. (a) A pre-scanned image. In which a-a and G are the grasping location and the

target position, respectively. (b) A post-manipulation image verifies that the manipulated SiNW is piled upon another nanowire deposited on the Si substrate

be seen that the SiNW has been successfully transported and piled onto another SiNW. The manipulation procedure is described as follows. Once the SiNW was reliably grasped, the piezoscanner moved down 560 nm at a velocity of 80 nm/s. In this step, the SiNW was transported a distance of 4.4 μm along the X-axis at a velocity of 120 nm/s and 0.12 μm along the Y-axis at a lower velocity of 3.3 nm/s. In the releasing step, the piezoscanner moved up at a velocity of 100 nm/s. As tip II was slightly bent upward leading to a positive response of 0.015 V, tip I and tip II were separated by moving both the nanostage and the piezoscanner on the X-axis to release the SiNW from the nanotip gripper.

Conclusion and Future Directions

A flexible robotic system developed for multi-scale manipulation and assembly from nanoscale to micro-scale is presented. This system is based on the principle of atomic force microscopy and comprises two individually functionalized cantilevers. After reconfiguration, the robotic system could be used for pick-and-place manipulation from nanoscale to the scale of several micrometers. Flexibilities and manipulation capabilities of the developed system are validated by pick-and-place manipulation of microspheres and silicon nanowires to build three-dimensional micro/nanostructures in ambient conditions.

Complicated micro/nano manipulation and assembly can be reliably and efficiently performed using the proposed flexible robotic system. 3-D nanomanipulation methods are indispensable for heterogeneous integration of complex nanodevices. Serial nanomanipulation systems could only enable low-volume prototyping applications. However, high-volume and high-speed nanomanipulation systems are indispensable for future nanotechnology products. Therefore, autonomous and massively parallel AFM systems are required.

Cross-References

- ▶ [AFM](#)
- ▶ [Atomic Force Microscopy](#)
- ▶ [Force Modulation in Atomic Force Microscopy](#)
- ▶ [Friction Force Microscopy](#)
- ▶ [Manipulating](#)
- ▶ [Nanogrippers](#)
- ▶ [Nanorobotic Assembly](#)
- ▶ [Nanorobotics](#)
- ▶ [Self-assembly of Nanostructures](#)

References

1. Menciassi, A., Eisinberg, A., Izzo, I., Dario, P.: From “macro” to “micro” manipulation: models and experiments. *IEEE-ASME Trans. Mechatro.* **9**(2), 311–320 (2004)
2. Lambert, P., Régnier, S.: Surface and contact forces models within the framework of microassembly. *J. Micromechat.* **3**(2), 123–157 (2006)
3. Sitti, M.: Microscale and nanoscale robotics systems-characteristics, state of the art, and grand challenges. *IEEE Robot. Autom. Mag.* **14**(1), 53–60 (2007)
4. Xie, H., Rong, W.B., Sun, L.N.: Construction and evaluation of a wavelet-based focus measure for microscopy. *Imaging Microsc. Res. Tech.* **70**, 987–995 (2007)
5. Liu, X.Y., Wang, W.H., Sun, Y.: Dynamic evaluation of autofocusing for automated microscopic analysis of blood smear and pap smear. *J. Microsc.* **227**, 15–223 (2007)
6. Xie, H., Rong, W.B., Sun, L.N., Chen, W.: Image fusion and 3-D surface reconstruction of microparts using complex valued wavelet transforms. In: *IEEE International Conference on Image Process*, Atlanta, pp. 2137–2140 (2006)
7. Xie, H., Vitard, J., Haliyo, S., Régnier, S.: Optical lever calibration in atomic force microscope with a mechanical lever. *Rev. Sci. Instrum.* **79**, 096101 (2008)
8. Xie, H., Rakotondrabe, M., Régnier, S.: Characterizing piezoscanner hysteresis and creep using optical levers and a reference nanopositioning stage. *Rev. Sci. Instrum.* **80**, 046102 (2009)
9. Vögeli, B., von Knel, H.: AFM-study of sticking effects for microparts handling. *Wear* **238**, 20–24 (2000)
10. Varenberg, M., Etsion, I., Halperin, G.: An improved wedge calibration method for lateral force in atomic force microscopy. *Rev. Sci. Instrum.* **74**, 3362–3367 (2003)
11. Xie, H., Vitard, J., Haliyo, S., Régnier, S.: Enhanced accuracy of force application for AFM nanomanipulation using nonlinear calibration of optical levers. *IEEE Sens. J.* **8**(8), 1478–1485 (2008)
12. Fukuda, T., Arai, F., Dong, L.X.: Assembly of nanodevices with carbon nanotubes through nanorobotic manipulations. *Proc. IEEE* **91**, 1803–1818 (2003)
13. Dong, L.X., Arai, F., Fukuda, T.: Electron-beam-induced deposition with carbon nanotube emitters. *Appl. Phys. Lett.* **81**, 1919–1921 (2002)
14. Dong, L.X., Arai, F., Fukuda, T.: Destructive constructions of nanostructures with carbon nanotubes through nanorobotic manipulation. *IEEE/ASME Trans. Mechatron.* **9**, 350–357 (2004)
15. Molhave, K., Wich, T., Kortschack, A., Boggild, P.: Pick-and-place nanomanipulation using microfabricated grippers. *Nanotechnology* **17**, 2434–2441 (2006)
16. Dong, L.X., Tao, X.Y., Zhang, L., Nelson, B.J., Zhang, X.B.: Nanorobotic spot welding: controlled metal deposition with attogram precision from copper-filled carbon nanotubes. *Nano Lett.* **7**, 58–63 (2007)
17. Leach, J., Sinclair, G., Jordan, P., Courtial, J., Padgett, M.J., Cooper, J., Laczik, Z.J.: 3D manipulation of particles into crystal structures using holographic optical tweezers. *Opt. Exp.* **12**, 220–226 (2004)
18. Yu, T., Cheong, F.C., Sow, C.H.: The manipulation and assembly of CuO nanorods with line optical tweezers. *Nanotechnology* **15**, 1732–1736 (2004)
19. Bosanac, L., Aabo, T., Bendix, P.M., Oddershede, L.B.: Efficient optical trapping and visualization of silver nanoparticles. *Nano Lett.* **8**, 1486–1491 (2008)
20. Rollot, Y., Régnier, S., Guinot, J.C.: Simulation of micro-manipulations: adhesion forces and specific dynamic models. *Int. J. Adhes. Adhes.* **19**, 35–48 (1999)

